

Modeling of zonal electrophoresis in plane channel of complex shape

Shiryayeva E. V.

Department of Mathematics, Mechanics and Computer Science,
Southern Federal University, 344090, Rostov-on-Don, Russia
shir@ns.math.rsu.ru

Vladimirov V. A.

Department of Mathematics, York University, York, YO10 5DD, UK
vv500@york.ac.uk

Zhukov M. Yu.

Department of Mathematics, Mechanics and Computer Science,
Southern Federal University, 344090, Rostov-on-Don, Russia
zhuk@ns.math.rsu.ru

Abstract

The zonal electrophoresis in the channels of complex forms is considered mathematically with the use of computations. We show that for plane S-type rectangular channels stagnation regions can appear that cause the strong variations of the spatial distribution of an admixture. Besides, the shape of an admixture zone is strongly influenced by the effects of electromigration and by a convective mixing. Taking into account the zone spreading caused by electromigration, the influence of vertex points of channel walls, and convection would explain the results of electrophoretic experiments, which are difficult to understand otherwise.

Keywords: Microchip, electrophoresis.

Introduction

During the last ten years or so the intense use of various microchips aimed to separate mixtures by an externally imposed electric field, to control micromixing and chemical reactions has been flourished (see *e.g.* [1, 2, 3, 4, 5, 6, 7, 8, 9, 10, 11, 12, 13, 14, 15, 16, 17, 18, 19, 20]). The industrial use of microchannels for the efficient separation of mixtures is well known as the technology called Lab-on-a-Chip. The most effective control of mass transfer in micro-fabricated fluid devices can be achieved with the use of electrokinetic phenomena such as electrophoresis and electroosmosis. The crucially important part of related research is computer modeling that helps to improve the design of microchips, to understand the processes involved, and to enhance experimental methods.

The modeling of the electrophoretic separation of a mixture represents a challenging problem due to the large number of physical phenomena involved into the mass transfer

driven by an electric field. One can count here such phenomena as diffusion, chemical reactions, dependence of electrical conductivity on concentrations, electroosmosis, Joule heat, convection, *etc.* It should be noticed that many papers devoted to the transport phenomena in microchannels take into account only diffusion, electroosmosis, and the Taylor-Aris dispersion. As the result these papers leave out of account some essential nonlinear effects that appear due to the dependence of electrical conductivity on component concentrations; it is well known that these effects significantly change zone shapes [21, 22, 23, 24, 25, 26] and even can trigger a so called substance-lock effect [27] (for an experimental verification see [28]).

The effects of electric field singularities that occur near the vertex points of electrophoretic chamber walls still have not been understood and mathematically described. For a simple case of a plane cross-shaped channel this singularity is of the order $\mathcal{O}(r^{-1/3})$, where r is a distance from the vertex point of the reflex angle $3\pi/2$. The related distortions of zone shapes are described in [29] and experimentally justified in [30]. In addition, transport processes can be effected by convective mixing, which can drastically deform the final stage of a separation process. The role of convection in electrophoresis is described in [31, 32, 33, 34, 35, 36]. It is apparent that one can weaken convection by the choosing of an appropriate orientation of a microchip in the gravity field. Nevertheless, taking convection into account can not be avoided for high precision experiments.

This paper is devoted to the computer modeling that reveals the effects of such key factors as vertex points of channel walls, electromigration, and convection on zone distortions. We present only the results of a small part of our numerical experiments that have been carried out with the use of a specially created interactive program for the modeling of zonal electrophoresis. The main result is the identifying of the parameter intervals when the distortions of moving zones are the most significant. These data can be very useful for the planning of new experiments and for the designing of electrophoretic chambers.

1 Mathematical Model

The mathematical models of electrophoresis (and in particular zonal electrophoresis) are well known [21, 26, 29, 37]. The dimensionless governing equations describing both the motion of separated (by the action of an electric field) substances and fluid convection (in the Oberbeck-Boussinesq approximation) are:

$$\frac{d\mathbf{v}}{dt} = -\nabla p + \mu\Delta\mathbf{v} - \mathbf{k} \sum_{k=1}^n \beta_k c_k, \quad \operatorname{div} \mathbf{v} = 0, \quad (1)$$

$$\frac{dc_k}{dt} + \operatorname{div} \mathbf{i}_k = 0, \quad \mathbf{i}_k = -\varepsilon|\gamma_k|\nabla c_k + \gamma_k c_k \mathbf{E}, \quad (2)$$

$$\mathbf{E} = -\nabla\varphi, \quad \mathbf{j} = \sigma\mathbf{E}, \quad \operatorname{div}(\sigma\nabla\varphi) = 0, \quad (\operatorname{div} \mathbf{j} = 0), \quad (3)$$

$$\sigma = \sigma_0 \left(1 + \sum_{k=1}^n \alpha_k c_k \right) > 0, \quad (4)$$

Here \mathbf{v} and p are velocity and pressure, \mathbf{E} and φ are the strength and the potential of an electric field, c_k is the k -th concentration ($k = 1, \dots, n$), \mathbf{i}_k — the flux of concentration, \mathbf{j} — the density of electric current, σ — mixture conductivity, σ_0 — the conductivity in the absence of admixtures (the conductivity of a buffer solution), μ — fluid viscosity, γ_k — electrophoretic mobility, β_k — the coefficient that appears in the linear dependence of density on concentration, α_k — the coefficient that appears in the linear dependence of conductivity on concentration, ε — characteristic diffusion coefficient ($\varepsilon|\gamma_k|$ are diffusion coefficients), \mathbf{k} — the unit vector of the z -axis that is anti-parallel to the gravity. The dimensionless variables used are described in [21, 29].

In the presented model the effects of Joule heat and electroosmosis have been neglected. The conductivity of a mixture has been modeled by the expression (4) that is natural for zonal electrophoresis; it is accepted that a mixture contains components with constant concentrations that represent so called buffer solution (such that at $c_k = 0$ its conductivity is σ_0). The concentrations of separated substances (samples) are assumed to be small enough. We should emphasize that the coefficients α_k can have different signs (positive or negative); from a physical viewpoint $\alpha_k < 0$ means that this particular substance has lower specific conductivity than that of a buffer solution. When this substance enters into a solution, it ‘replaces’ the buffer substances and the conductivity of a mixture is decreasing (for details see [21, 24, 25, 37]).

Let us consider the domain shown in Fig. 1.1. We accept that its boundary is rigid with non-leak conditions for a liquid and for the concentrations c_k

$$\mathbf{v} = 0, \quad \mathbf{i}_k \cdot \mathbf{n} = 0, \quad k = 1, \dots, n. \quad (5)$$

where \mathbf{n} is the unit vector to the boundary.

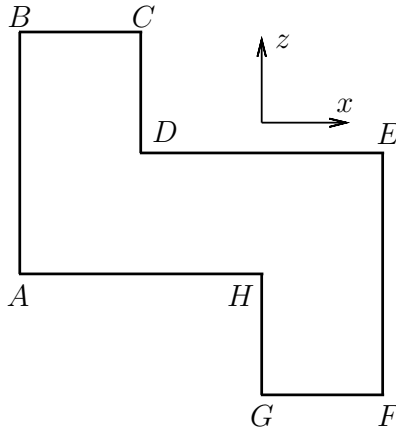


Figure 1.1: Electrophoretic chamber

The potential φ is prescribed on the parts BC and GF , while the rest of the boundary is insulated:

$$\varphi|_{BC} = \varphi_0, \quad \varphi|_{GF} = \varphi_1, \quad (6)$$

$$\left. \frac{\partial \varphi}{\partial n} \right|_{CDEF,BAHG} = 0. \quad (7)$$

At the initial instant a fluid is still and the initial distributions of admixtures are prescribed:

$$\mathbf{v}|_{t=0} = 0, \quad c_k|_{t=0} = c_k^0(x, z), \quad k = 1, \dots, n. \quad (8)$$

2 Qualitative Analysis of the Problem

There are at least four factors that influence the distortion of a zone as well as admixture concentrations. The first one is diffusion that causes the spreading of electrophoretic zones. For small concentrations (the case of analytical electrophoresis) nonlinear effects are weak and diffusion makes the separation of admixtures difficult; its influence is well studied and described in almost all handbooks on zonal electrophoresis (see [21, 37]). The second factor is the electromigration spreading of zones. It reveals itself for high concentrations (for example for preparative electrophoresis) and described in details in [21, 25, 26]. Recall, that in one-dimensional case the evolution of an initially rectangular concentration profile for a single admixture follows the patterns shown in Fig. 2.1 where two upper pictures give initial distributions for positive and negative α_1 , while two bottom pictures present some later stages of their developments.

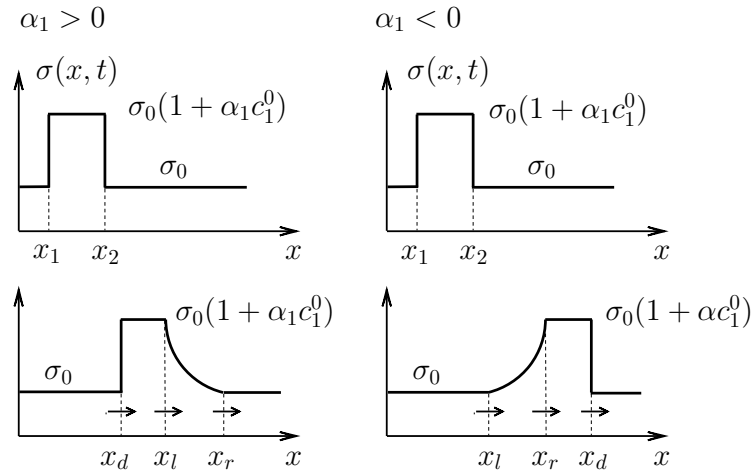


Figure 2.1: The zone evolution

The analysis of diffusionless ($\varepsilon = 0$) quasi-linear conservative hyperbolic laws (2)–(4) in one-dimensional case with $\mathbf{v} = 0$ shows that for $\alpha_k < 0$ a shock wave $x = x_d(t)$ at the

forward part of concentration profile c_k is formed. Simultaneously there are two fronts of rarefaction wave $x = x_l(t)$ and $x = x_r(t)$ that appear at the backward part of the profile. The velocities of these shock wave and the fronts of rarefaction wave are constants:

$$V_d = \frac{\gamma_1}{1 + \alpha_1 c_1^0}, \quad V_l = \gamma_1, \quad V_r = \frac{\gamma_1}{(1 + \alpha_1 c_1^0)^2}, \quad \alpha_1 < 0. \quad (9)$$

The conductivity in the rarefaction wave is:

$$\sigma = \sigma_0 \left(\frac{\gamma_1 t}{x - x_1} \right)^{1/2}, \quad x_l(t) \leq x \leq x_r(t). \quad (10)$$

In contrast, for the case $\alpha_k > 0$ there is a shock wave $x = x_d(t)$ at the backward part of the profile and there are two fronts of rarefaction wave $x = x_l(t)$ and $x = x_r(t)$ on the forward part of the profile. The distributions shown in Fig. 2.1 do exist until the instant $t = t_{\text{int}}$, when a direct interaction between the waves takes place. For example, for $\alpha_k < 0$ the front of rarefaction wave $x_r(t)$ will catch up with the shock wave $x_d(t)$ *i.e.* $x_r(t_{\text{int}}) = x_d(t_{\text{int}})$. The further evolution can be described analytically. Omitting details, one can notice that finally the concentration profile adapts a ‘triangular’ shape (Fig. 2.2).

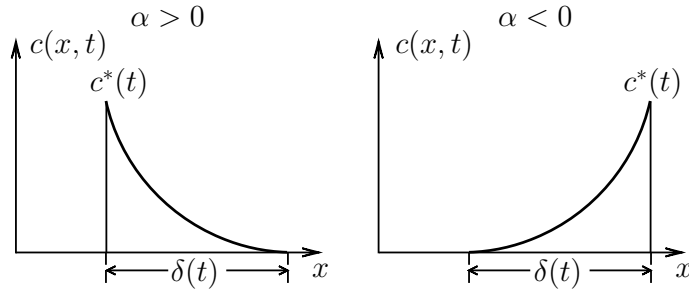


Figure 2.2: Final stage of the process

At $t \rightarrow +\infty$ the height $c^*(t)$ and the base $\delta(t)$ of the ‘triangle’ are given (independently of the sign of α) as

$$c^*(t) \sim \left(\frac{M}{\alpha_1 \gamma_1 t} \right)^{1/2}, \quad \delta(t) \sim 2 (\alpha_1 \gamma_1 M t)^{1/2}, \quad \frac{1}{2} c^*(t) \delta(t) \sim M = c_1^0 (x_2 - x_1), \quad (11)$$

where M is the total mass of an admixture. Notice that the ‘spreading’ of the concentration in the absence of diffusion process is:

$$c^*(t) = \mathcal{O}(t^{-1/2}), \quad \delta(t) = \mathcal{O}(t^{1/2}), \quad t \rightarrow +\infty$$

It represents a nonlinear effect of electromigration spreading that takes place due to the dependence of the admixture transfer velocity on the concentration. Notice that in the case of conventional diffusion $c^*(t)$ and $\delta(t)$ are changing similarly; that is the reason why experimentalists often mix up these two very different phenomena (diffusion and hyperbolic

spreading of a concentration profile); at the same time one should take into account that the spreading due to diffusion is much slower than hyperbolic spreading (constants in the similar laws are very different!). More details on the zone evolution the zonal electrophoresis are given in [21, 25, 26, 27]. The two-dimensional version of this problem can be solved only numerically but we can still analytically derive that there is a shock wave of concentration on the forward part of the profile and a rarefaction wave of concentration at the rear part of a wave for $\alpha < 0$. A normal coordinate to a zone boundary corresponds to the x -direction in one-dimensional case.

The third factor causing the distortions of a zone reveals itself only for the domains with vertex points where the singularities of electric potential take place. In the simplest case when admixtures are absent (pure buffer solution) and a fluid is still ($\mathbf{v} = 0$, $c_k = 0$, $\sigma = \sigma_0$), the equation $\text{div } \mathbf{j} = 0$ produces Laplace's equation for the potential $\Delta\varphi = 0$ with the boundary conditions (6), (7). In the vicinity of the vertex of the angle α there is a solution $\varphi = Ar^{\pi/\alpha} \cos(\pi\theta/\alpha)$ where (r, θ) are polar coordinates with the origin at a vertex. One can see that the gradient of such a potential possesses a singularity $\nabla\varphi = \mathcal{O}(r^{\pi/\alpha-1})$. In particular, for the domain shown in Fig. 1.1 the radial component of electric field E_r at the points D and H ($\alpha = 3\pi/2$) is very large: $E_r = \mathcal{O}(r^{-1/3})$. In contrary, at points A and E ($\alpha = \pi/2$) the singularities are absent and the electric field is small: $E_r = \mathcal{O}(r)$. Now, let all admixture at the initial instant be placed in the vicinity of BC and the potential difference $\varphi_1 - \varphi_0$ be such that the migration of admixture is directed towards GF . It is apparent that there is a fast admixture transport in the vicinities of points D and H , and a slow one in the vicinities of A and E . In the latter case the formation of stagnation regions is likely. This effect will eventually cause the strong distortion of zone shapes.

Finally, the fourth factor is gravitational concentration convection. The difference between the densities of an admixture and a buffer fluid generates buoyancy flows in the regions of inhomogeneous density. One can guess that there should be an intense fluid flow induced by the motion of an admixture in the vicinities of points D and H (see Fig. 1.1).

3 Numerical Experiments

The problem (1)–(7) has been solved by a direct simulation with the employing of the finite-difference method of markers and cells (MAC). In order to approximate the transport equations (2) we have used combined explicit and implicit finite-difference schemes with the finite differences taken in the direction opposite to a flow; the latter allows us to block mesh diffusion effects. To compute the flow velocity \mathbf{v} we have used explicit schemes. Finally the method of ‘sequence over relaxation’ (SOR) with the relaxation parameter $1.37 \div 1.96$ has been chosen for the computation of pressure p and potential φ (in the solving of finite-difference analogues of elliptic equations). It should be noticed that due to singularities in $\nabla\varphi$ in the vicinities of points D and H the SOR method has been essentially modified: in particular we introduced five subdomains with the appropriate matching conditions at their

boundaries. In addition, the computations have also been carried out by the finite element method with the use of FreeFem++ and FlexPDE. The comparative relative error between the computations by the different methods used has been below 0.03.

The initial concentration is prescribed in a circular zone of radius r centered at x_0, z_0 as

$$c^0(x, z) = \frac{1}{2} \left(1 + \tanh(-\delta((x - x_0)^2 + (z - z_0)^2 - r^2)) \right),$$

or in a rectangular zone given by an appropriate expression. Both these distributions represent ‘almost step functions’ with the parameter $\delta = 100$ used for the smoothing of discontinuities.

3.1 Zone Distortion in Complex Shape Channel

Some typical results for the channel shown in Fig. 1.1 are presented in Fig. 3.1–3.3. In the case of a lighter single admixture ($\mu = 0.01, \beta_1 = -0.1, \gamma_1 = -0.15, \varphi_1 - \varphi_0 = 20, \alpha_1 = -0.4, \varepsilon = 0.1$) the surface levels of the concentration $c_1(x, z)$ and the streamlines of fluid flows are shown in Figs. 3.1, 3.2. The sequence of frames 1–6 corresponds to the instants $t = 0.24, 9.91, 14.66, 26.71, 42.11, 68.50$. The potential difference chosen drives the zone from the line BC towards the line GF . The lengths of intervals in the channel boundary $ABCDEFGH$ are:

$$|BC| = w_1 > 0, |DE| = 1 - w_1 > 0, |GF| = w_2 > 0, |AH| = 1 - w_2 > 0, \quad w_1 = w_2 = \frac{1}{3},$$

$$|CD| = h_1 > 0, |HG| = h_2 > 0, |AB| = 1 - h_2 > 0, |EF| = 1 - h_1 > 0, \quad h_1 = h_2 = \frac{1}{3}.$$

Combined explicit and implicit schemes have allowed us to use the mesh 60×60 with rather large steps $h_x = h_y = 0.0167$. It is well visible that there are strong distortions of the zone shape in the vicinities of points D, H , while in the vicinities of the points A, E the admixture is retarded in stagnation regions. It is interesting that the distortion is so strong that it causes the formation of three vortices (for the instant $t = 14.66$ in the frame 3, Fig. 3.2) in the vicinity of the point D and the subsequent disappearing of one vortex.

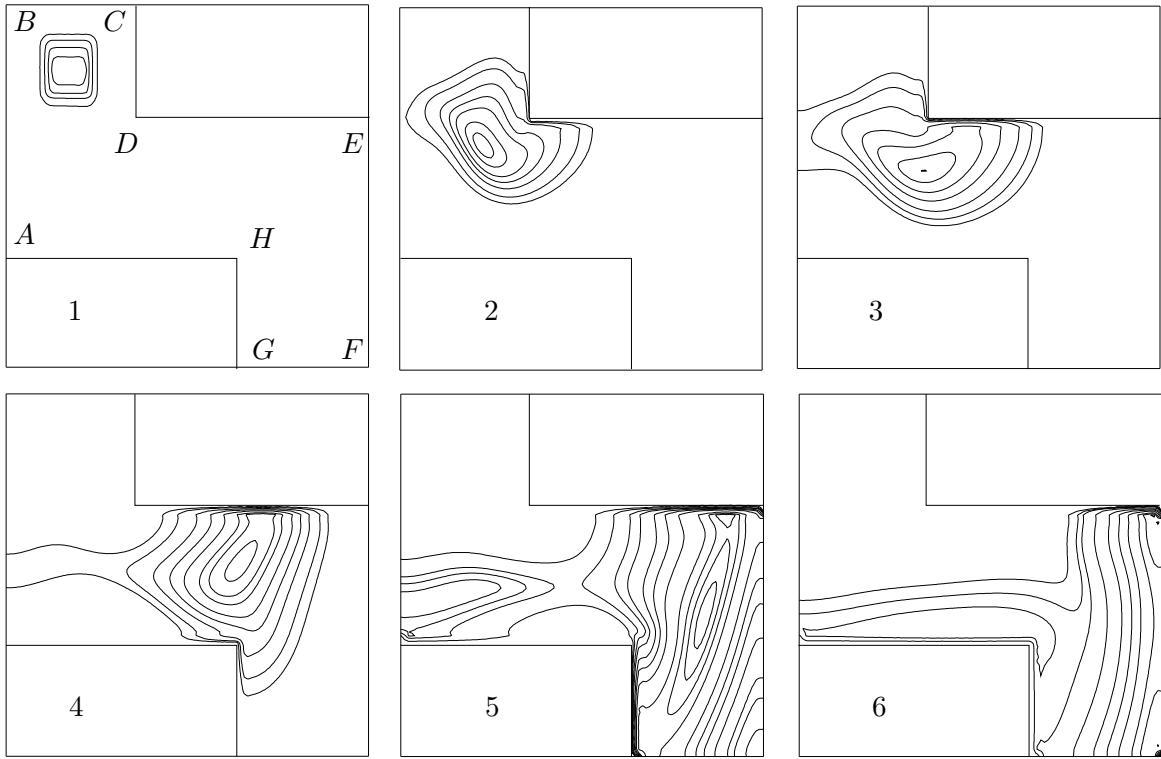


Figure 3.1: The surface levels of concentration $c_1(x, z, t)$

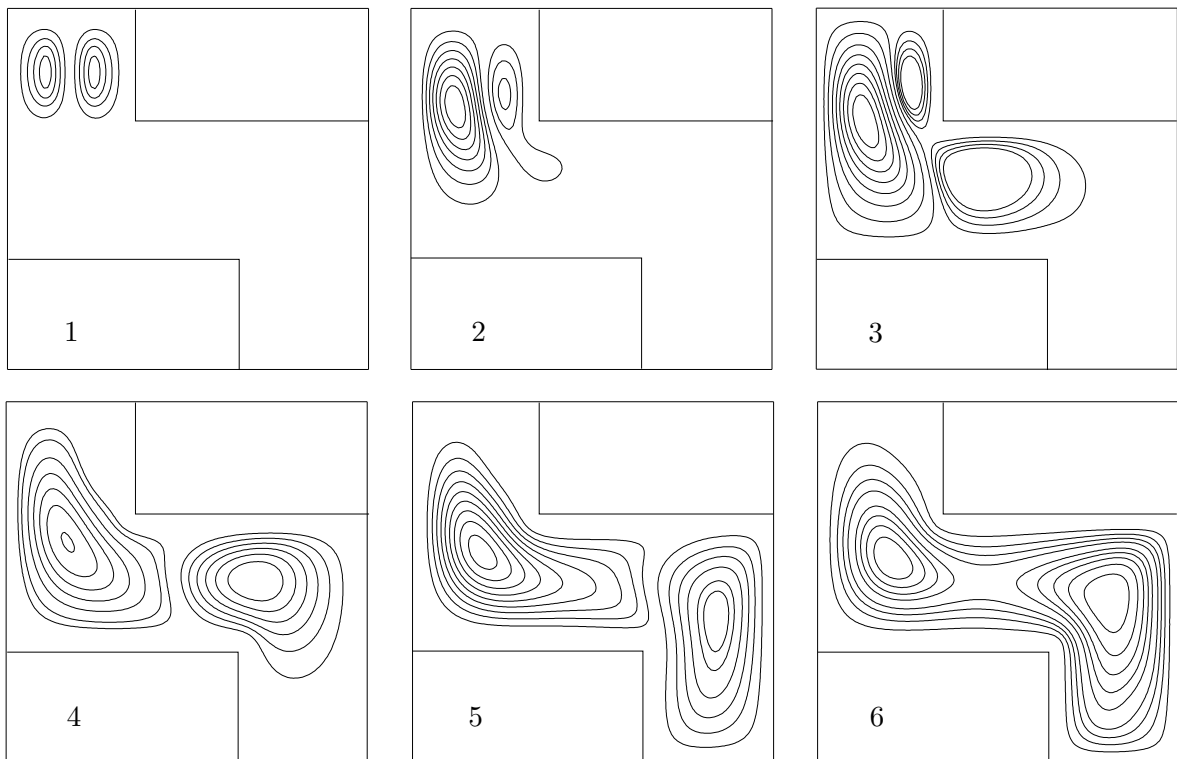


Figure 3.2: The streamfunction

The numerical experiments have shown that the variations of the diffusion parameter ε

within the interval ($0.0001 < \varepsilon < 0.1$) does not change the results. It means that electromigration (not diffusion!) is the main reason for the zone spreading, while diffusion can affect the deforming of zone only in large time intervals. A series of computations have shown that qualitatively similar pictures with the forming of stagnation regions and the distortion of a zone shape have been observed in a wide interval of ε . The changing of $|\gamma_1||\varphi_1 - \varphi_0|$ (for the fixed μ, β_1) leads only to the changing of a time scale for the zone passing through the channel. The typical size of a zone in the direction of motion (before its qualitative distortion has appeared) has been defined by the parameter α_1 . It agrees well with the results for one-dimensional case (see Figs. 2.1, 2.2) at least for $\alpha_1 > -0.5$. The zone distortion is most sensible to the change of the parameters h_1, h_2, w_1, w_2 that prescribe the relative sizes of an electrophoretic chamber. Any quantitative description of a zone distortion is rather difficult. For ‘symmetric’ chambers with $0.05 < h_1 = h_2 < 0.1$ and $0.05 < w_1 = w_2 < 0.1$ up to 40% of the total mass of an admixture is trapped in the vicinity of points A and E , while for the case $0.3 < h_1 = h_2 < 0.4$ and $0.2 < w_1 = w_2 < 0.3$ this figure is up to 25%. The intensity of convection is strongly influenced by the viscosity μ or more precisely by $\text{Gr} = |\beta_1\mu^{-2}|$, where Gr is a version of Grashof’s number related to concentration. An intense (almost chaotic) mixing takes place for $\text{Gr} > 10^8$.

The frames 1 and 2, Fig. 3.3 show a stage of the separation of two admixtures that are heavier than the buffer ($\mu = 0.01, \varepsilon = 0.1, \varphi_1 - \varphi_0 = 20, \beta_1 = 0.1, \beta_2 = 0.1, \gamma_1 = -0.15, \gamma_2 = -0.35, \alpha_1 = -0.4, \alpha_2 = -0.4$). It is interesting to see that the ‘faster’ admixture ($|\gamma_2| > |\gamma_1|$) has been undergoing the larger distortions. We have split the pictures for two concentrations into two frames in order to avoid visual superimposing of surface levels. The frame 3, Fig. 3.3 shows a stage of separation of two heavier admixtures moving in the opposite directions (towards each other) ($\mu = 0.01, \varepsilon = 0.1, \varphi_1 - \varphi_0 = 20, \beta_1 = 0.1, \beta_2 = 0.1, \gamma_1 = -0.15, \gamma_2 = 0.15, \alpha_1 = -0.4, \alpha_2 = -0.4$). It is noticeable that the motion of the admixture c_2 against the gravity causes the greater profile distortions than the motion of the admixture $c_1(x, z)$ along the gravity field.

The described numerical experiments have shown that the motion of zones in the gravity field and in channels with vertex points does produce very strong zone distortions. This fact explains the failures of the experiments with the ‘Kashtan’ devices in space that were noticed in [29, 30].

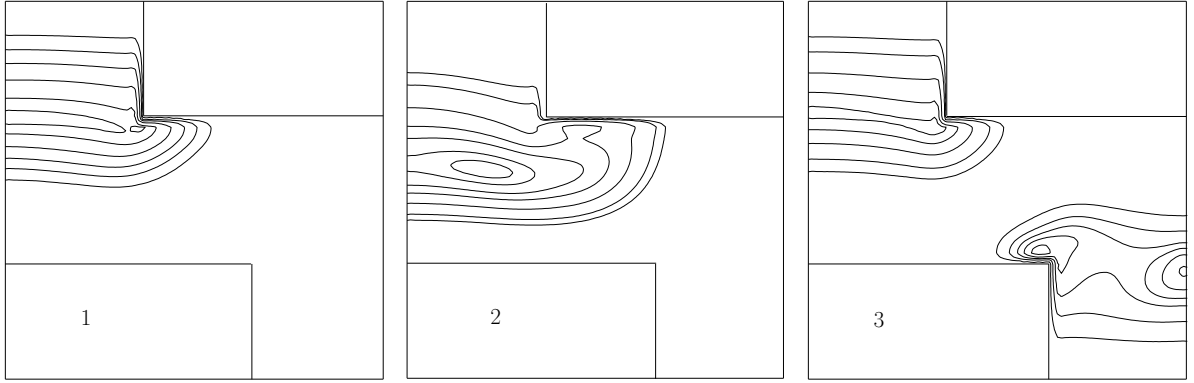


Figure 3.3: The surface levels of the concentrations $c_1(x, z)$ (frame 1), $c_2(x, z)$ (frame 2), and $c_1(x, z)$, $c_2(x, z)$ (frame 3)

3.2 Zone Distortion in Rectangular Channel

In order to demonstrate more clearly the influence of convective mixing on the zone distortion we have also made computations for a simple rectangular channel where the singularities of an electric field are absent. Constant potentials has been prescribed on side walls, while top and bottom walls has been insulated. The width of the channel is $a = 2$, while its height is $b = 1$. The rest of parameters have been chosen as: $\varphi_1 - \varphi_0 = 20$, $\mu = 0.01$, $\gamma_1 = -0.35$, $\varepsilon = 0.01$. Below we present the results for a single admixture with different values α_1 and β_1 which show that the gravity can strongly affect the admixture transport via the buoyancy driven intense vortex flows near the zone.

Figs. 3.4, 3.5 present the surface levels for $\beta_1 = -200$ (a lighter admixture) in a fluid with small viscosity ($\text{Gr} = 2 \cdot 10^6$) for two different values of α_1 at the instants $t = 0.0256$; 0.1024 ; 0.1792 ; 0.2304 where one can clearly see electromigration spreading. For $\alpha_1 < 0$ (Fig. 3.4) the forward front exhibits the compression of surface levels (a shock wave), while the rear front — a rarefaction wave. For $\alpha_1 > 0$ (Fig. 3.5) those features are opposite: the rear front represents a shock wave, while the forward front — a rarefaction wave. These results have been in agreement with the properties of motion in one-dimensional case (see Figs. 2.1, 2.2). Notice that the zone form has been essentially distorted at the initial stages of motion. The buoyancy effects at $\beta_1 = -200$ are very weak; the admixture is slightly moving upwards while it is transported by an electric field.

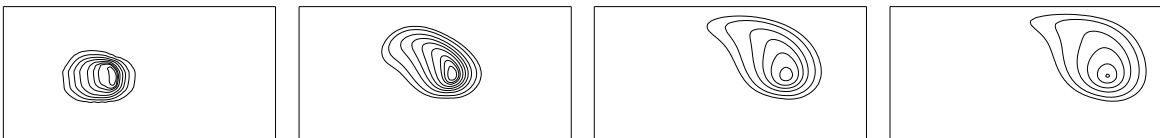


Figure 3.4: The surface levels. $\alpha_1 = -0.4$

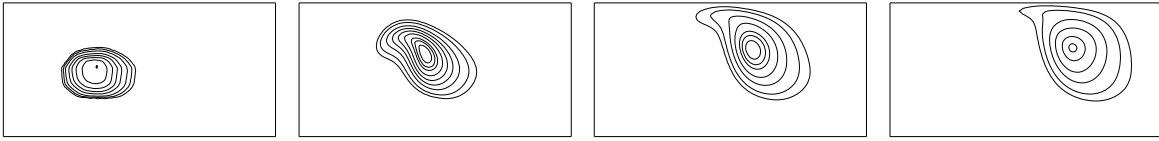


Figure 3.5: The surface levels. $\alpha_1 = 0.4$

Fig. 3.6 corresponds to $\alpha_1 = -0.4$. It shows the surface levels of concentrations at the instants $t = 0.0512$; 0.1024 ; 0.1280 . Here we have chosen the admixture being five times lighter ($\beta_1 = -1000$, $\text{Gr} = 2 \cdot 10^7$) than in the previous case of Figs. 3.4, 3.5; so the influence of the gravity here is quite essential. One can clearly see the strong interaction of the arising zone with the upper wall that causes the apparent splitting of a single zone into two (Fig. 3.6). The next Fig. 3.7 demonstrates the correspondent streamline pictures that reveal the forming of a vortex pair in the process of convective mixing. These results show that the gravity can change the zone shape drastically.

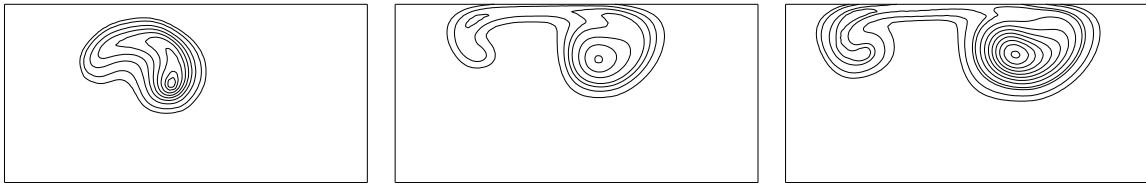


Figure 3.6: The surface level of concentration

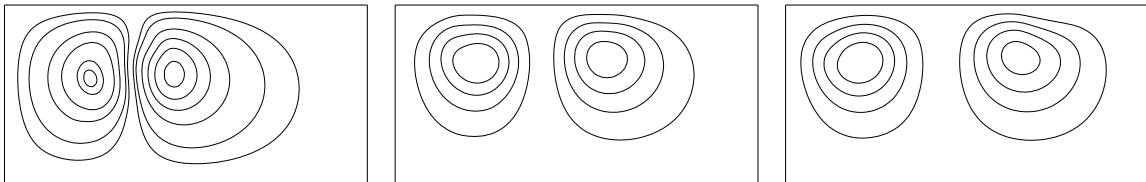


Figure 3.7: The streamlines

Acknowledgments

This research is partially supported by EPSRC (research grants GR/S96616/01, EP/D055261/1, and EP/D035635/1), by the Russian Ministry of Education (programme ‘Development of the research potential of the high school’, grants 2.1.1/6095 and 2.1.1/554), and by Russian Foundation for Basic Research (grants 07-01-00389, 08-01-00895, and 07-01-92213 NCNIL). The authors are grateful to the Department of Mathematics of the University of York for the providing of excellent conditions for this research.

References

- [1] Kaniansky, D.; Masar, M.; Bodor, R.; Zuborova, M.; Olvecka, E.; Johnck, M.; Stanislawski, B. *Electrophoresis*. **2003**, *24* (12–13), 2208–2227.
- [2] Erickson, D.; Liu, X.; Krull, U. J.; Li, D. *Anal. Chem.* **2004**, *76*, 7269–7277.
- [3] Bharadwaj, R.; Santiago, J. G.; Mohammadi, B. *Electrophoresis*. **2002**, *23*, 2729–2744.
- [4] Molho, J. I.; Herr, A. E.; Mosier, B. P.; Santiago, J. G.; Kenny, Th. W. *Anal. Chem.* **2001**, *73*, 1350–1360.
- [5] Jen, C.; Wu, C.; Lin, Y.; Wu, C. *Lab Chip*. **2003**, *3*, 77–81.
- [6] Johnson, T. J.; Ross, D.; Locascio, L. E. *Anal. Chem.* **2002**, *74*, 45–51.
- [7] Berli, C. L. A.; Piaggio, M. V.; Deiber, J. A. *Electrophoresis*. **2003**, *24* (10), 1587–1595.
- [8] Chen, C.-H.; Santiago, J. G. In Proc. *IMECE*; 2002, *1* (33563).
- [9] Erickson, D.; Li, D. *Langmuir*. **2003**, *19*, 5421–5430.
- [10] Ermakov, S. V.; Jacobson, S. C.; Ramsey, J. M. In Tech. Proc. of the Int. Conference on Modeling and Simulation of Microsystems MSM 99; U.S.A., 1999; pp. 534–537.
- [11] Ermakov, S. V.; Jacobson, S. C.; Ramsey, J. M. *Anal. Chem.* **1998**, *70*, 4494–4504.
- [12] Ermakov, S. V.; Jacobson, S. C.; Ramsey, J. M. *Anal. Chem.* **2000**, *72*, 3512–3517.
- [13] Ghosal, S. *Electrophoresis*. **2004**, *25* (2), 214–228.
- [14] Guijt, R. M.; Evenhuis, C. J.; Macka, M.; Haddad, P. R. *Electrophoresis*. **2004**, *25* (23–24), 4032–4057.
- [15] Herr, A. E.; Molho, J. I.; Drouvalakis, K. A.; Mikkelsen, J. C.; Utz, P. J.; Santiago, J. G.; Kenny, Th. W. *Anal. Chem.* **2003**, *75*, 1180–1187.
- [16] Hu, Y.; Werner, C.; Li, D. *Anal. Chem.* **2003**, *75*, 5747–5758.
- [17] Oddy, M. H.; Mikkelsen, J. C.; Santiago, J. G. *Anal. Chem.* **2001**, *73*, 5822–5832.
- [18] Patankar, N. A.; Hu, H. H. *Anal. Chem.* **1998**, *70* (9), 1870–1881.
- [19] Patankar, N. A.; Santiago, J. G. *Anal. Chem.* **2005**, *77*, 6672–6781.
- [20] Santiago, J. G. *Anal. Chem.* **2001**, *73*, 2353–2365.
- [21] Babskii, V. G.; Zhukov, M. Yu.; Yudovich, V. I. *Mathematical theory of electrophoresis*; Plenum Publishing Corporation: New York, 1989.

- [22] Zhukov, M. Yu.; Yudovich, V. I. *Soviet Physics Doklady*. **1982**, *27*, 918–924.
- [23] Zhukov, M. Yu. *J. Comp. math. and math. phys.* **1984**, *24* (4), 549–565 (in Russian).
- [24] Ermakov, S. V.; Zhukov, M. Yu.; Righetti, P. G. *Electrophoresis*. **1996**, *17*, 1134–1142.
- [25] Bello, M. S.; Zhukov, M. Yu.; Righetti, P. G. *J. Chrom. A*. **1995**, *693*, 113–130.
- [26] Zhukov, M. Yu. *Mass transfer in an electric field*; Rostov University Press: Rostov-on-Don, 2005.
- [27] Zhukov, M. Yu.; Ermakov, S. V.; Righetti, P. G. *SIAM J. Appl. Math.* **1999**, *59* (2), 743–776.
- [28] Ermakov, S. V.; Zhukov, M. Yu.; Capelli, L.; Righetti, P. G. *Anal. Chem.* **1994**, *66*, 4034–4042.
- [29] Babskii, V. G.; Zhukov, M. Yu.; Myshkis, A. D.; Kopachevskii, N. D.; Slobozhanin, L. A.; Tyuptsov, A. D. *Methods of Solving Problems of Hydromechanics in Zero Gravity*; Naukova Dumka: Kiev, 1992.
- [30] Zhukov, M. Yu.; Babskii, V. G.; Sazonov, L. I.; Stoyanov, A. V. *Space science and technology*. **1989**, *4*, 15–19 (in Russian).
- [31] Bello, M. S.; Polezhaev, V. I. *Fluid Dynamics*. **1990**, *2*, 14–20 (in Russian).
- [32] Polezhaev, V. I.; Bello, M. S.; Verezub, N. A. *Convection in zero gravity*. Nauka: Moscow, 1991 (in Russian).
- [33] Zhukov, M. Yu.; Tsyvenkova, O. A. *Fluid Dynamics*. **1994**, *29* (5), 717–723.
- [34] Zhukov, M. Yu.; Tsyvenkova, O. A. *Fluid Dynamics*. **1995**, *30* (5), 652–660.
- [35] Zhukov, M. Yu.; Petrovskaya, N. V. *Fluid Dynamics*. **1997**, *32* (5), 631–641.
- [36] Zhukov, M. Yu.; Sazonov, L. I. *Diff. Uravn.* **1997**, *3* (4), 470–477 (in Russian).
- [37] Mosher, R. A.; Saville, D. A.; Thorman, W. *The dynamics of electrophoresis*; VCH Publishers: New York, 1992.